International Journal of Electrical, Electronic and Communication Sciences
ISSN: 2517-9438
Vol:11, No:11, 2017

# Oil Recovery Study by Low Temperature Carbon Dioxide Injection in High-Pressure High-Temperature Micromodels

Zakaria Hamdi, Mariyamni Awang

***Abstract*—**For the past decades, $CO_2$ flooding has been used as a successful method for enhanced oil recovery (EOR). However, high mobility ratio and fingering effect are considered as important drawbacka of this process. Low temperature injection of $CO_2$ into high temperature reservoirs may improve the oil recovery, but simulating multiphase flow in the non-isothermal medium is difficult, and commercial simulators are very unstable in these conditions. Furthermore, to best of authors' knowledge, no experimental work was done to verify the results of the simulations and to understand the pore-scale process. In this paper, we present results of investigations on injection of low temperature $CO_2$ into a high-pressure high-temperature micromodel with injection temperature range from 34 to 75 °F. Effect of temperature and saturation changes of different fluids are measured in each case. The results prove the proposed method. The injection of $CO_2$ at low temperatures increased the oil recovery in high temperature reservoirs significantly. Also, $CO_2$ rich phases available in the high temperature system can affect the oil recovery through the better sweep of the oil which is initially caused by penetration of $LCO_2$ inside the system. Furthermore, no unfavorable effect was detected using this method. Low temperature $CO_2$ is proposed to be used as early as secondary recovery.

***Keywords*—**Enhanced oil recovery, $CO_2$ flooding, micromodel studies, miscible flooding.

## I. Introduction

$CO_2$ injection is being applied as a successful tertiary recovery method for the last decades, especially in the form of water alternating gas (WAG) process to overcome the gravity override and early breakthrough. Several WAG processes are done during the years and reported thoroughly [1]-[3]. For each reservoir, based on the temperature, pressure, and the composition of the crude oil, a miscibility pressure is defined. If the miscibility between the gas phase (i.e. $CO_2$) and the crude oil is formed, high recovery is expected [4], [5]. While in general, immiscible flooding results in lower recovery factor [6], [7]. Recent studies suggest that when using liquid $CO_2$, it will cause the minimum miscibility pressure (MMP) to be almost independent of molecular weight and MMP will decrease by decreasing temperature [8]. In addition, numerous core flooding displacement tests are designed and performed to optimize different $CO_2$ flooding scenarios [9]-[11]. Other than field pilots and laboratory experiments, numerical simulations were done, trying to find better solutions which match with experimental results [12], [13]. However, simulating multiphase flow in the non-isothermal medium is difficult, and studies have shown that commercial simulators are very unstable under these conditions [14]. In recent studies, it was suggested that using $CO_2$ with temperatures lower than critical temperature (i.e. °88 F), leads to better sweeping efficiency and also limits the unfavorable mobility of gases [2]. This may result in the lower need to water flooding which can improve the reservoirs performance.

Micromodels are etched glasses with artificial nature, that are generally used for pore-scale studies. The usage of micromodels goes back to over 50 years for fluid displacement investigation [15]. The main advantage of micromodel usage is when multiple phases interact with each other. They helped the development of network models in multiphase flow [16]-[18]. A few micromodel studies are done aiming for $CO_2$ flooding [13], [14], [19], [20]. Further development of the pore-scale modeling is described in detail by Sohrabi et al. [20].

In this paper, we investigate the usage of low temperature $CO_2$ injection under high-pressure high-temperature micromodel and its effect on oil recovery obtained from different injection temperatures.

## II. Objective

The main objective of this study is to evaluate the usage of low temperature $CO_2$ injection and its effectiveness in high temperature systems. The pressure and temperature of the micromodel are set so that immiscible flooding is expected. Then, the effect of low temperature $CO_2$ injection on miscibility is studied. The effect of injection temperature is expected to have a direct impact on oil recovery.

## III. Methodology

To obtain the objective of the study, a unique high pressure micromodel is designed in which liquid $CO_2$ can be injected in high pressure high temperature micromodel without any breakage of the equipment. This equipment is able to record the saturation, interactions and overall oil recovery in different pressure and temperatures of both reservoir (micromodel) and injection fluid. Although the results cannot be applicable to field size because of its 2D nature, it can validate previous simulations which are done to evaluate the effectiveness of this method [1], [2], [21]. Different scenarios of immiscible

Zakaria Hamdi is with Heriot-Watt University, Malaysia (corresponding author, phone: 60126303254; e-mail: H.Zakaria@hw.ac.uk).
Mariyamni Awang is a Professor with Elsa Energy, Malaysia (e-mail: Mari.Awang@elsa-energy.com).

and miscible as well as secondary and tertiary recovery are performed in order to verify the viability of the proposed method. If the data obtained are in tally with the previous results, then this method can be suggested to be implemented in field scale simulations and finally in field pilots.

### A. Experimental Equipment

For performing low temperature $CO_2$ flooding, a unique high pressure high temperature micromodel is designed and used. The experiments were carried out at pressures of 700-2400 psi, and the micromodel temperature was kept constant at 140 °F, covering immiscible and miscible flooding. The injection temperature range was from 34 to 75 °F. A schematic diagram of the equipment is in Fig. 1.

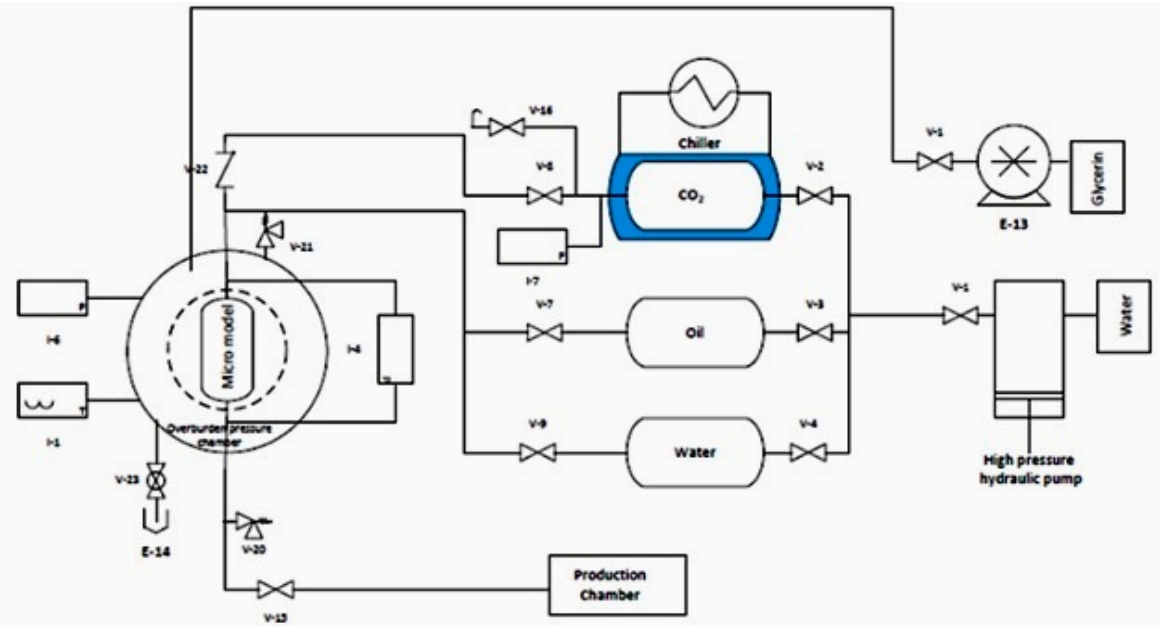


Fig. 1 A schematic diagram of micromodel equipment

This micromodel setup consists of several parts. A very low flow rate pump was used in the system having a very high accuracy (up to 10-5 ml/min). The rate of injection was kept constant at 0.002 ml/min which is equivalent to the speed of 3 ft/day. Also, three high pressure accumulators used to contain $CO_2$, crude oil, and water. A cubic stainless steel chamber is designed to ensure high pressure capability of the system. Two acrylic windows are put on the top and bottom of the chamber due to the capability of the light passage through the chamber to visualize the flooding in the micromodel. A built-in heater is available inside the chamber in order to maintain the temperature required for the micromodel glass. In order to perform the experiment at high pressures, a confining pressure is required maintain the outside pressure of glass micromodel. This pressure has to be precisely controlled since a slight pressure difference (100 psi) may lead to breakage of the micromodel glass. The difference is kept at 35 psi in all time, which is enough to avoid any overpass of the injected fluids. This pressure is controlled by a high pressure water pump which is automatically controlled by the PC. A chiller and a tank are used to obtain a low temperature medium. The $CO_2$ accumulator is placed in the tank at all times. The isolation of the system allows $CO_2$ to enter the micromodel at desired temperature which is as low as 34 °F in this study. Micromodel glass consists of an etched glass that is used as a 2D pore structure. The pores are controlled but randomly generated and distributed forming homogeneous medium. The etching process and controlled generation of the pores are available in the previous literature [22]. A cover glass is used to form a closed pore space. The two glasses are then covered by two acrylic plates for higher strength against pressure change. The inlet and outlet are at the two ends of the glass. They are also etched on the micromodel glass, allowing displacement of the fluids through the micromodel. Due to very shallow depth of the etching part (which is equal to one pore), it is possible to consider the pattern as a 2D pore model representing the reservoir. The micromodel is placed horizontally and therefore, no gravity override may take place. A magnified picture of the etched micromodel is shown in Fig. 1. The size of the medium is 31 mm in width and 80 mm in length, while the depth is around 0.08 mm. The pore throat is approximately 0.15 mm while the pore radius is 1.7 mm. the total pore volume of the micromodel is approximately 0.09 $cm^3$. All of the glasses are put into a bracket for further strength.

Since the micromodel studies data are mainly derived from the visualization of the micromodel glass, it is vital to use a proper optical system for image capturing. The system includes a controlled light source located at the bottom of the micromodel chamber and a macro zoom camera at the top of

the chamber. The camera can move slightly along the micromodel to ensure coverage of the whole picture of the micromodel glass. The pictures taken from the camera can be later analyzed by pixel-counting software based on the color of the pixels. As a result, the saturations of each of the fluid can be measured with acceptable precision. Finally, since the displaced volume is very small, the back pressure regulator needs to be modified. Instead of the traditional valve system used, a Nitrogen-filled accumulator is used as back pressure to avoid any pulse into the system. It can be pressurized according to the experiment pressure and it can be used as a fluid collector. The pressure is controlled through the PC along with injection and confining pressure.

### *B. Experimental Fluids*

For $CO_2$ flooding experiments, three fluids have been used. A light crude oil sample is colored red using Sudan Red dye. The MMP for this crude is obtained in previous studies as 1934 psi at 140 °F. The distilled water is colored blue by Methyl Blue dye and placed in the accumulator. The 99.99% purified $CO_2$ is used as flooding agent. No major preparation is needed for water and crude oil since a built-in filter is used in the system to avoid any unwanted blockage inside the micromodel. $CO_2$ is pressurized separately while lowering the temperature to the desired. An equilibration time of 4 hours is considered to ensure the liquefied $CO_2$ temperature reached the aimed temperature.

## IV. Results and Discussion

A total of 22 experiments were done using different pressures and injection temperature. For each run, a general cleaning and preparation process is done. First, the micromodel is filled with crude oil and pressurized up to the desired point. After reaching the desired pressure and constant temperature of 140 °F, an extended water flood is done. In this point, the average water and oil saturation were recorded 83.1% and 16.9%, respectively. Then the experiment is followed by injection of crude oil. By initial testing, it is observed that after 3 pore volumes of crude oil injection, the fluid saturations remain the same and no further changes in water and oil saturations are observed. Therefore, in order to make same conditions for all of the experiments, 3-pore volume is considered as the reference point to provide the initial crude oil and water. This injection represents the migration of the oil into the reservoir while having initial water. At this point, the micromodel is ready for the main displacements. A magnified section of the micromodel in this stage is shown in Fig. 2. This picture is less than 5% of the whole micromodel, yet representing the whole micromodel. During several experiments done in this stage, the initial saturations were recorded as an average of 11.3% (Swi) and 88.7% (Soi) for water and oil, respectively (±2% for both fluids).

As the injection rate was kept constant (0.002 ml/min) during different injection schemes and exceeding 2.5 pore volume of $CO_2$ injection, it was observed that the changes in saturations of different phases were negligible. Therefore, this displacement amount is fixed for all of the experiments. For water flooding cases, the same rate and amount are considered. Since the whole etched pores are too small to be visible with naked eye, the fluid saturations can only be measured by pixel count. Magnified sections of an immiscible and a miscible flooded micromodel samples (less than 5% of the micromodel) are shown in Figs. 3 and 4, respectively.

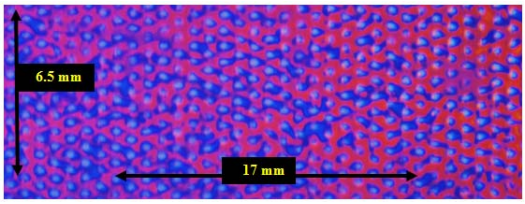


Fig. 2 A section of the micromodel at initial conditions showing initial oil and water saturations in red and blue, respectively (Soi = 88.7% and Swi = 11.3%)

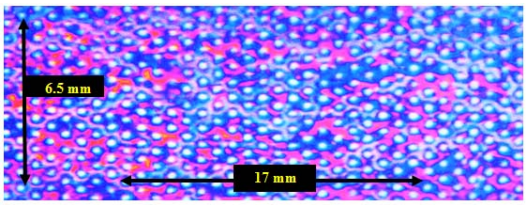


Fig. 3 A sample of immiscible $CO_2$ flooding in the micromodel, showing residual oil, gas and water saturations in red, white, and blue, respectively

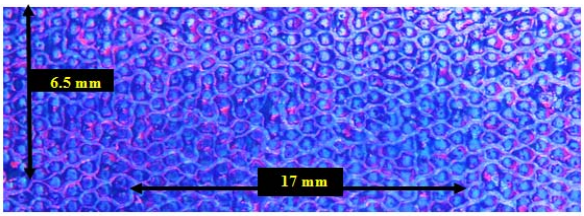


Fig. 4 A sample of miscible $CO_2$ flooding in the micromodel, showing a very good sweep by $CO_2$

Considering the temperature and pressure conditions explained in the previous chapter, 19 $CO_2$ flooding displacements are done, and saturations are recorded at the end of experiments. A 20$^{th}$ case is considered as a water flooding case, followed by two cases of $CO_2$ injection at a different temperature as tertiary recovery. All of the micromodel results experiments are presented in Table I.

The MMP is expected to be higher since red dye solved in crude oil will likely act as an impurity and may increase the MMP significantly [23]. Therefore, 2400 psi is taken as a reliable miscible flooding and immiscible flooding is appears in pressures below 1900 psi.

The saturations were calculated using analysis of the images taken at the end of the experiments which were categorized by blue, red, and white color pixels for water, oil, and gas respectively. Fluid saturations were plotted against temperature in different pressures to investigate the effect of

injection temperature on saturations and consequently on the recovery.

TABLE I
RESULTS OF INJECTION OF $CO_2$ AT VARIOUS TEMPERATURES AND PRESSURES INTO THE MICROMODEL WITH 140 °F INITIAL TEMPERATURE

| Exp. No | P (psi) | Injection Condition (based on micromodel initial conditions) | $T_{inj}$ (°F) | $S_{gr}$ % | $S_{wr}$ % | $S_{or}$ % | RF % |
|---|---|---|---|---|---|---|---|
| 1 | 2400 | Miscible | 75 | 73.2 | 9.1 | 17.7 | 80.05 |
| 2 | 2400 | Miscible | 68 | 73.1 | 9 | 17.9 | 79.82 |
| 3 | 2400 | Miscible | 59 | 77 | 9 | 14 | 84.22 |
| 4 | 2400 | Miscible | 50 | 83.3 | 8.8 | 7.9 | 91.09 |
| 5 | 2400 | Miscible | 41 | 86.7 | 8.7 | 4.6 | 94.81 |
| 6 | 2400 | Miscible | 34 | 88.1 | 8 | 3.9 | 95.60 |
| 7 | 1900 | Near Miscible | 75 | 58.9 | 9.2 | 31.9 | 64.04 |
| 8 | 1900 | Near Miscible | 68 | 69.5 | 9.3 | 21.2 | 76.10 |
| 9 | 1900 | Near Miscible* | 59 | 76.8 | 9.1 | 14.1 | 84.10 |
| 10 | 1900 | Near Miscible* | 50 | 81.9 | 8.8 | 9.3 | 89.52 |
| 11 | 1900 | Near Miscible* | 41 | 82.4 | 8.8 | 8.8 | 90.08 |
| 12 | 1900 | Near Miscible* | 34 | 83.3 | 8.6 | 8.1 | 90.87 |
| 13 | 1600 | Immiscible | 75 | 52.6 | 9.4 | 38 | 57.16 |
| 14 | 1600 | Immiscible | 50 | 53 | 9.2 | 37.8 | 57.38 |
| 15 | 1600 | Immiscible* | 41 | 76.1 | 9.1 | 14.8 | 83.31 |
| 16 | 1600 | Immiscible* | 34 | 83.2 | 8.5 | 8.3 | 90.64 |
| 17 | 1200 | Immiscible | 75 | 50.2 | 9.4 | 40.4 | 54.45 |
| 18 | 1200 | Immiscible | 34 | 58.9 | 9.4 | 31.7 | 64.26 |
| 19 | 700 | Immiscible | 34 | 47 | 9.8 | 43.2 | 51.30 |
| 20 | 2400 | Water Flooding | 75 | 0 | 61.6 | 38.4 | 56.71 |
| 21 | 2400 | Water Flooding followed by $CO_2$ | 75 | 63.4 | 15.4 | 21.2 | 76.10 |
| 22 | 2400 | Water Flooding followed by $CO_2$ | 34 | 72.2 | 13.6 | 14.2 | 83.99 |

*Injection of CO2 at the specified temperature changed the marked cases to miscible flooding

First, the water saturation is monitored to see the effect of injection temperature of $CO_2$ on water saturation. Constant water saturation usually leads to better recovery. As seen from the table, decreasing the injection temperature leads to a slight decrease of water saturation (~1%). Also, increasing the pressure causes lower water saturation. For cases 21 and 22 where water flooding is used first, the residual water saturation is 4 to 5% higher than other cases. This was normal as in the two cases, higher water saturation was present before $CO_2$ flooding is done.

As for the water saturations, the results show that in micro scale, there is not much change in water saturation when using $CO_2$ as the flooding agent and the initial water remain almost intact. In the investigated range, the change in water saturation was less than 2%. The visual findings show that $CO_2$ is likely to interact with oil phase and it will not sweep the water phase.

Gas saturation change is shown in Fig. 5. Gas saturation is detected by the white (colorless) part of the photo taken from the micromodel.

Gas saturation for low pressures (700 and 1200 psi) at all tested temperatures is below 60%, confirming an immiscible flooding (considering constant water saturation). Excluding the point at 75 °F and 1900 psi, high pressure $CO_2$ injection will result in higher gas saturation. The excluded point has a lower than 60% saturation at 75 °F and 1900 psi, because it is quite near to formation of miscibility with the oil, some of the gas is still in the oil phase and not released and pushed the oil away yet. The gas saturation in tertiary flooding cases is considerably lower in compare with $CO_2$ injection as a secondary recovery method. The reason is because of more water available inside the system in tertiary flooding. As a result, less gas can be present in the micromodel.

The oil saturation is calculated using red pixels of the photos at the end of each experiment. The oil saturation is likely to be an over-estimation as there may be some gas miscible with the oil which is yet counted as oil. The oil saturation is plotted as Fig. 6.

As seen, for each pressure, decreasing the temperature results in lower oil saturation. Also, for each temperature, increasing pressure will decrease the oil saturation. Even in 1600 psi and 50 °F, which has a considerably high oil saturation, it still can be considered as the same trend as this point lies in the miscibility region of the crude oil. As a result, it is expected that the gas is in a single phase with the oil and with a proper time, the gas dissolved in the oil would come out the oil and the saturation would become less. The most notable fact in this figure is that comparing the 2400 psi cases, one can verify the benefit of using miscible flooding as secondary recovery other than tertiary, which results in lower oil saturation in favor of $CO_2$ injection as the secondary flooding.

Using the oil saturations of different experiments and considering initial oil saturation, the recovery factor can be obtained as in Fig. 7.

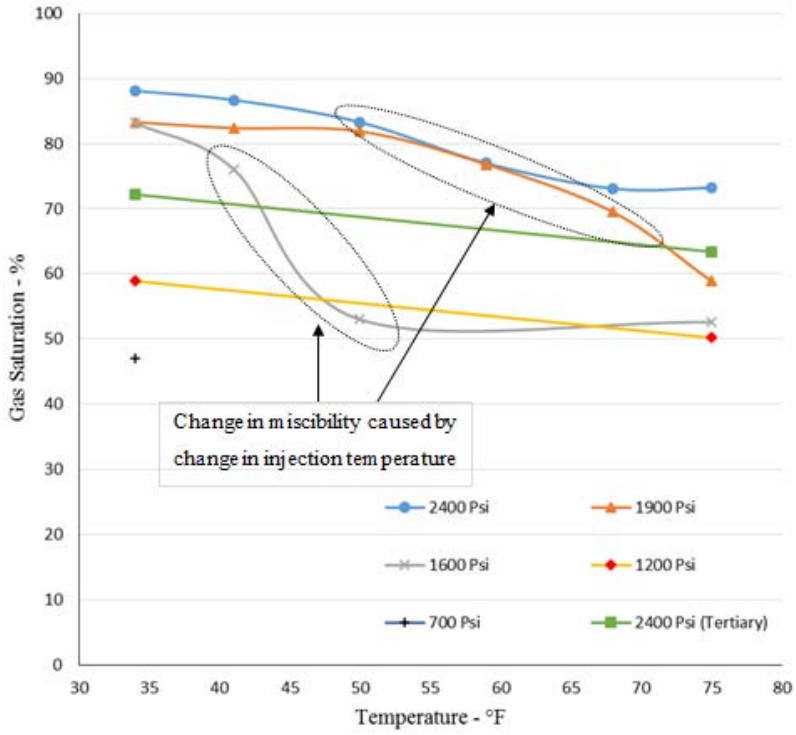


Fig. 5 Gas saturation vs. injection temperature for each injection pressure

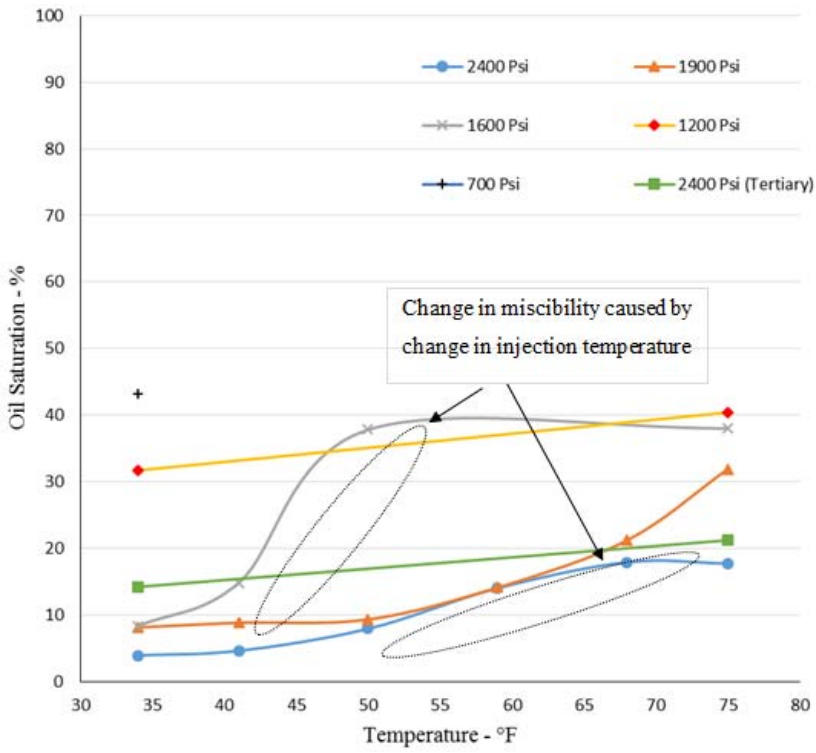


Fig. 6 Oil saturation vs. injection temperature for each injection pressure

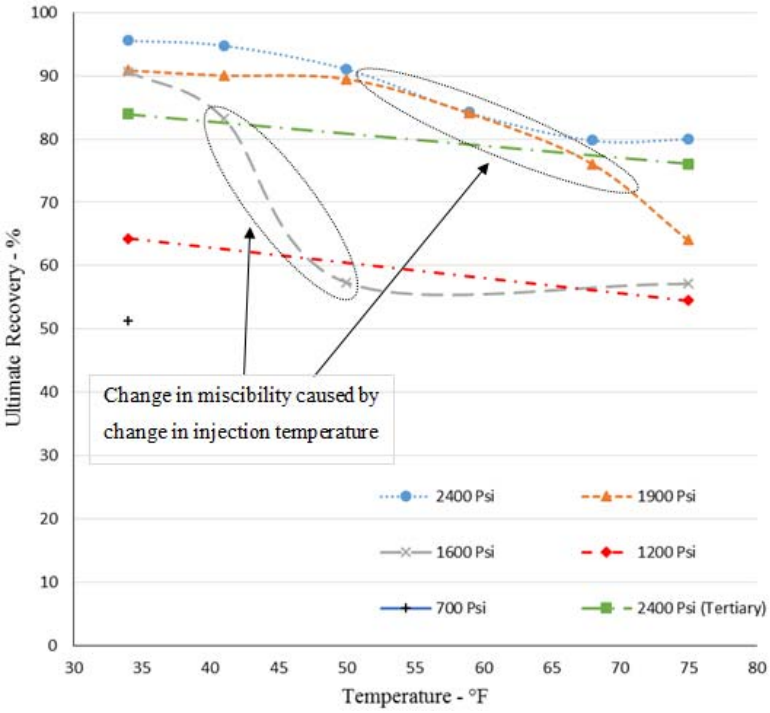


Fig. 7 Recovery factor vs. temperatures in different pressures

As expected in miscible flooding displacements, high recovery factors were observed in the pressures above 1900 psi, confirming a miscible displacement. When the pressure is 1900 psi and 75 F temperature injection was conducted, the phases were miscible. As a result, the colored part which is counted for oil saturation is over-estimated. Therefore, the gas which is miscible with the crude oil (counted as oil saturation) caused the recovery factor amount to be an under-estimation. As a result, the displacement should be considered to be near miscible although the recovery is displaced less than 70%.

The effect of temperature can be seen in the line of 1600 psi, where temperature decrease at low temperature region will cause a miscible displacement. In pressures lower than 1600 psi, immiscible displacement occurred, as expected.

During the displacement, it is observed that at low temperature injections, some of the $LCO_2$ (brighter white than $CO_2$) penetrates further into the micromodel, then suddenly dissolves into the oil as shown in Fig. 8. This shows the ability of $LCO_2$ to form miscible flooding which can penetrate further inside. The presence of $LCO_2$ also shows that the temperature is brought down locally. As the injection continues, more $LCO_2$ penetrates into the micromodel and as a result, $LCO_2$ exists further into the micromodel.

Different phases were observed during miscible flooding at low temperatures, especially when injection temperature was 34 °F. The water phase was distinct showing a blue color, while the colorless $CO_2$ phase was white due to the light. Two oil phases were observed. One was dark red in color showing an oil phase, while the other one was formed near $LCO_2$, representing high concentration $CO_2$ in the oil phase, having a light orange color. This phase was in agreement with previous studies that observed $CO_2$ rich phase when using low temperature medium [20]. This phase was then separated into two phases of $CO_2$ and oil before reaching the end of the micromodel. The reason is the temperature increase of the front in the micromodel and as a result, losing multiple contacts between $CO_2$ and crude oil at the micromodel conditions. As discussed before, an $LCO_2$ phase (bright white) was distinguished in the process which later on vanished into the oil forming the $CO_2$ rich phase. This phase is responsible for forming miscibility with the oil in regions that gaseous $CO_2$ is not able to do so since the higher pressure was needed for gaseous $CO_2$ to form miscibility.

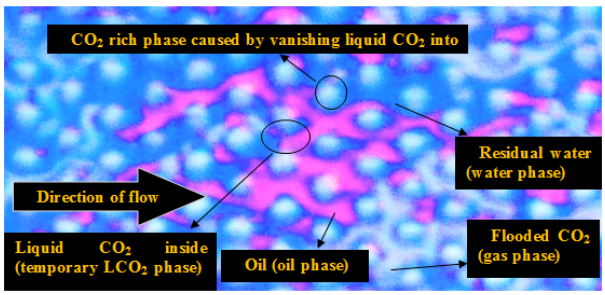


Fig. 8 Presence of $LCO_2$ inside the micromodel among other phases before vanishing and forming a single phase into the oil

The results of the micromodel experiments showed that although it was not possible to measure the temperature along the micromodel, the temperature varied inside the micromodel, depending on the injection temperature and the distance from the injection point. As a result, lower

temperature $CO_2$ injection leads to the formation of miscibility with the crude oil along the micromodel while the initial conditions of the micromodel predicted an immiscible flooding. At the interaction regions during the low temperature $CO_2$ injection, an additional phase ($LCO_2$ phase) is present that is different from the gaseous $CO_2$ phase. This phase is temporary as it vanishes into the oil once it becomes gas phase. When it vanishes among the crude oil, it forms a $CO_2$ rich phase. The latest phase is responsible for increase the sweeping efficiency as the viscosity of the crude oil decreases which results in better movement. The proposed method can be beneficial especially in the areas that have huge low temperature $CO_2$ supply such as cryogenic separation units.

## V. Conclusion

The results presented in this study improved our knowledge in low temperature $CO_2$ flooding. The multiphase flow and presence of liquid $CO_2$ inside high temperature micromodel open the opportunity for field scale applicability of the proposed method. The results showed that different injection temperature did not have any effect on the residual water saturation. While lower injection temperature led to better sweep efficiency. Our micromodel observations prove that liquid $CO_2$ exists in the high pressure high temperature micromodel. Liquid $CO_2$ expansion inside the micromodel caused the better penetration inside the pore, which results in a better invasion of the residual oil by $CO_2$. Additionally, the miscibility between $CO_2$ and the crude oil is formed at pressures lower than the expected MMP which obtained before. This result proves the ability of liquid $CO_2$ to locally reduce the miscibility pressure. Overall result shows that difference in temperature could increase the oil recovery by 30% more than gaseous injection of $CO_2$. However, due to 2D nature of the micromodel, the gravity override is neglected in this study.

## Nomenclature

P: Pressure (Psi)
Tinj: Temperature (°F)
Sgr: Residual Gas Saturation (%)
Swr: Residual Water Saturation (%)
Sor: Residual Oil Saturation (%)
RF: Recovery Factor (%)

## Acknowledgment

Authors would like to thank Center of Research in Enhanced Oil Recovery, Universiti Teknologi PETRONAS for their support. They wish to extend their regards to Universiti Teknologi PETRONAS for funding the equipment construction.

## References

[1] Z. Hamdi and M. Awang, "Improving Oil Recovery by Cold CO2 Injection: A Simulation Study," International Journal of Petroleum and Geoscience Engineering (IJPGE), vol. 1, pp. 167-177, 30/09/2013 2013.
[2] Z. Hamdi, M. Bt. Awang, and B. Moradi, "Low Temperature Carbon Dioxide Injection in High Temperature Oil Reservoirs," presented at the International Petroleum Technology Conference, 2014.
[3] J. R. Christensen, E. H. Stenby, and A. Skauge, "Review of WAG Field Experience," SPE Reservoir Evaluation & Engineering, vol. 4, pp. 97-106, 04/01/2001 2001.
[4] S. Elgaghah, A. Y. Zekri, R. A. Almehaideb, and S. A. Shedid, "Laboratory Investigation of Influences of Initial Oil Saturation and Oil Viscosity on Oil Recovery by CO2 Miscible Flooding," presented at the EUROPEC/EAGE Conference and Exhibition, London, U.K., 2007.
[5] S. Chen, H. Li, D. Yang, and P. Tontiwachwuthikul, "Optimal Parametric Design for Water-Alternating-Gas (WAG) Process in a CO2-Miscible Flooding Reservoir," 2010/10/1/.
[6] A. Spivak, W. H. Garrison, and J. P. Nguyen, "Review of an Immiscible CO2 Project, Tar Zone, Fault Block V, Wilmington Field, California," SPE Reservoir Engineering, vol. 5, pp. 155-162, 05/01/1990 1990.
[7] T. D. Ma and G. K. Youngren, "Performance of Immiscible Water-Alternating-Gas (IWAG) Injection at Kuparuk River Unit, North Slope, Alaska."
[8] Z. Hamdi and M. Awang, "CO2 Minimum Miscibility Pressure Determination of Pure Hydrocarbons in Different Temperatures Using Slimtube Simulations," Research Journal of Applied Sciences, Engineering and Technology, vol. 7, pp. 3159-3163, 2014.
[9] L. Minssieux, "WAG Flow Mechanisms in Presence of Residual Oil", Society of Petroleum Engineers. doi:10.2118/28623-MS, 1994
[10] A. Y. Zekri and A. A. Natuh, "Laboratory Study of the Effects of Miscible WAG Process on Tertiary Oil Recovery."
[11] J. R. Christensen, E. H. Stenby, and A. Skauge, "Compositional and Relative Permeability Hysteresis Effects on Near-Miscible WAG."
[12] J. A. Larsen and A. Skauge, "Simulation of the Immiscible WAG Process Using Cycle-Dependent Three-Phase Relative Permeabilities."
[13] M. I. J. v. Dijke, M. Lorentzen, M. Sohrabi, and K. S. Sorbie, "Pore-Scale Simulation of WAG Floods in Mixed-Wet Micromodels," SPE Journal, vol. 15, pp. pp. 238-247, 03/01/2010 2010.
[14] M. Sohrabi, D. H. Tehrani, A. Danesh, and G. D. Henderson, "Visualisation of Oil Recovery by Water Alternating Gas (WAG) Injection Using High Pressure Micromodels - Oil-Wet & Mixed-Wet Systems," presented at the SPE Annual Technical Conference and Exhibition, New Orleans, Louisiana, 2001.
[15] c. c. a. K. Mattax, j.r., "Ever see waterflood?," Oil & Gas Journal, vol. 59, 1961.
[16] R. Lenormand, C. Zarcone, and A. Sarr, "Mechanisms of the displacement of one fluid by another in a network of capillary ducts," Journal of Fluid Mechanics, vol. 135, pp. 337-353, 1983.
[17] M. Blunt and P. King, "Relative permeabilities from two- and three-dimensional pore-scale network modelling," Transport in Porous Media, vol. 6, pp. 407-433, 1991/08/01 1991.
[18] J. A. Billiotte, H. De Moegen, and P. Oren, "Experimental Micromodeling and Numerical Simulation of Gas/Water Injection/Withdrawal Cycles as Applied to Underground Gas Storage," 1993/4/1/.
[19] M. Sohrabi, G. D. Henderson, D. H. Tehrani, and A. Danesh, "Visualisation of Oil Recovery by Water Alternating Gas (WAG) Injection Using High Pressure Micromodels - Water-Wet System," presented at the SPE Annual Technical Conference and Exhibition, Dallas, Texas, 2000.
[20] M. Sohrabi, D. H. Tehrani, A. Danesh, and G. D. Henderson, "Visualization of Oil Recovery by Water-Alternating-Gas Injection Using High-Pressure Micromodels," SPE Journal, vol. 9, pp. 290-301, 09/01/2004 2004.
[21] Z. Hamdi, M. Awang, & A. Zamani, "Evaluating Liquid CO2 Injection Technique for Oil Recovery Using Core Flood Experiments", Society of Petroleum Engineers. doi:10.2118/184092-MS, 2016.
[22] S. G. Sayegh and D. B. Fisher, "Enhanced Oil Recovery by CO2 Flooding in Homogeneous and Heterogeneous 2D Micromodels," Journal of Canadian Petroleum Technology, vol. 48, pp. 30-36, 08/01/2009 2009.
[23] P. Y. Zhang, S. Huang, S. Sayegh, and X. L. Zhou, "Effect of CO2 Impurities on Gas-Injection EOR Processes," 2004.